

Dynamic Compression of Porous Tungsten*

R. R. BOADE

Sandia Laboratories, Albuquerque, New Mexico 87115

(Received 28 February 1969; in final form 9 April 1969)

Data are presented from a study conducted to examine the shock-loading behavior of a sintered porous tungsten with a density of 12.64 g/cm^3 (corresponding to 65.3% of the density of solid tungsten). The experiments were performed by using a gas gun and high explosives. Hugoniot data obtained in the stress range between about 12 kbar and 1 Mbar indicate that compression of the porous material to a fully compacted state is essentially complete at 50 kbar. Above this level, a predicted Hugoniot, calculated from the Hugoniot of solid tungsten by using the Mie-Grüneisen equation of state, agrees well with experimental data. Below 50 kbar the Hugoniot of the porous tungsten deviates from the predicted Hugoniot increasingly with decreasing stress. Propagated wave profiles at lower stresses are characterized by two precursor waves, the faster being a low-level wave ($\sim 0.2 \text{ kbar}$) traveling at about sonic velocity in the porous tungsten ($\sim 3.04 \text{ mm}/\mu\text{sec}$). The slower precursor has an amplitude of 2.73 kbar and travels at $2.02 \text{ mm}/\mu\text{sec}$. The behavior of this porous tungsten is analogous to the behavior of sintered porous copper previously studied.

INTRODUCTION

Recent experimental studies^{1,2} conducted to examine the behavior of porous materials under shock loading have shown that Hugoniots of these materials can be predicted quite accurately for cases where the amplitude of the input-stress wave is sufficient to cause complete compaction. These predictions have been made by using the known dynamic properties of the solid portions of the porous material in conjunction with the Mie-Grüneisen equation of state. At lower input stresses, Hugoniots of porous materials deviate from the predicted Hugoniots increasingly as the stress level is decreased.²⁻⁴ Propagated disturbances at low stresses are generally found to be complex, with one or more precursor waves being present. The properties of these precursor waves depend on the basic properties of the solid material and/or on the manner in which the porous material is fabricated. For example, in a study of pressed iron powder, Lysne and Halpin³ observed a single precursor wave propagating with constant velocity and amplitude. This wave, however, was not formed on impact but appeared to emanate from the main shock wave after a short distance of travel. A different phenomenon was observed in a study of sintered porous copper.² Here, two precursor waves were observed, each of which formed immediately and propagated with constant velocity and amplitude. The velocity of the first precursor wave was approximately equal to the longitudinal sound velocity in the porous copper and the velocity of the second precursor was about half the sonic velocity.

The work reported in the present paper is based on an experimental study of the shock-loading behavior of

sintered porous tungsten with a density of 12.64 g/cm^3 . This density corresponds to 65.3% of the density of solid tungsten (19.3 g/cm^3). The microstructure of the porous tungsten studied here is similar to that of the sintered porous copper studied earlier. The porosity of both materials is due to the presence of many small ($< 0.001 \text{ mm}$ in diam), noninterconnecting pores uniformly distributed throughout the materials. The objectives of this work were to examine in detail the structure of the propagated disturbances at low input stresses and also to determine the Hugoniot of this material at both low and high stresses, i.e., in the regions of both incomplete and complete compaction. The low-stress experiments were performed on a gas gun and the high-stress experiments were performed using explosives.

The results of the experiments are similar to those of the sintered porous copper study in that at low stresses two precursor waves followed by a stronger shock wave were observed. Throughout this paper the two precursor waves will be referred to as the first and second waves and the final wave will be referred to as the third or main wave.

EXPERIMENTAL TECHNIQUES

The experimental techniques and data-reduction methods used in this study are essentially the same as those described in Ref. 2 so only the modifications pertinent to this study will be discussed in detail.

The gas-gun experiments were performed by impacting a flat-faced projectile (faced with quartz, Lucalox, or a porous tungsten sample) on a porous tungsten sample that was backed with a quartz gauge^{5,6} for recording the profile of the transmitted wave. The target assemblies were fabricated by one of two methods.

* This work was supported by the U.S. Atomic Energy Commission.

¹ R. G. McQueen, S. P. Marsh, and W. J. Carter, Dynamic High Pressure Conference, Paris (1967).

² R. R. Boade, *J. Appl. Phys.* **39**, 5693 (1968).

³ P. C. Lysne and W. J. Halpin, *J. Appl. Phys.* **39**, 5488 (1968).

⁴ R. K. Linde and D. N. Schmidt, *J. Appl. Phys.* **37**, 3259 (1966).

⁵ W. J. Halpin, O. E. Jones, and R. A. Graham in "Symposium on Dynamic Behavior of Materials," ASTM Special Tech. Publ. No. 336 (1963).

⁶ G. A. Jones and W. J. Halpin, *Rev. Sci. Instrum.* **39**, 258 (1968).

TABLE I. Data obtained for first two waves in 12.64 g/cm³ porous tungsten.

| Projectile facing | Projectile velocity (mm/ μ sec) | Sample thickness (mm) | P_{1Q}^a (kbar) | t_1^b (μ sec) | P_{2Q}^c (kbar) | t_2^d (μ sec) |
|-------------------|-------------------------------------|-----------------------|-------------------|----------------------|-------------------|----------------------|
| Quartz | 0.184 | 3.05 | 0.15 | 1.05 | 1.96 | 1.49 |
| Quartz | 0.201 | 1.91 | 0.10 | 0.61 | 1.77 | 0.91 |
| Quartz | 0.242 | 3.06 | 0.15 | 1.04 | 2.12 | 1.50 |
| Quartz | 0.271 | 1.02 | 0.15 | 0.35 | 3.15 | 0.66 |
| Quartz | 0.271 | 1.92 | 0.13 | 0.67 | 1.80 | 1.10 |
| Quartz | 0.301 | 3.06 | 0.12 | 1.01 | 1.98 | 1.59 |
| Quartz | 0.351 | 1.04 | 0.20 | 0.35 | 3.03 | 0.69 |
| Quartz | 0.350 | 1.91 | 0.11 | 0.61 | 1.68 | 0.90 |
| Quartz | 0.350 | 3.07 | 0.15 | 0.99 | 1.96 | 1.57 |
| Tungsten | 0.242 | 3.07 | 0.13 | 1.09 | 1.80 | 1.74 |
| Tungsten | 0.459 | 4.06 | 0.13 | 1.33 | 1.83 | 1.96 |
| Lucalox | 0.397 | 3.27 | 0.35 | 1.10 | 2.09 | 1.57 |
| Lucalox | 0.449 | 3.27 | 0.10 | 0.97 | 1.79 | 1.39 |
| Lucalox | 0.499 | 3.27 | 0.45 | 1.09 | 1.96 | 1.59 |
| Lucalox | 0.549 | 3.27 | 0.15 | 0.97 | 1.48 | 1.45 |

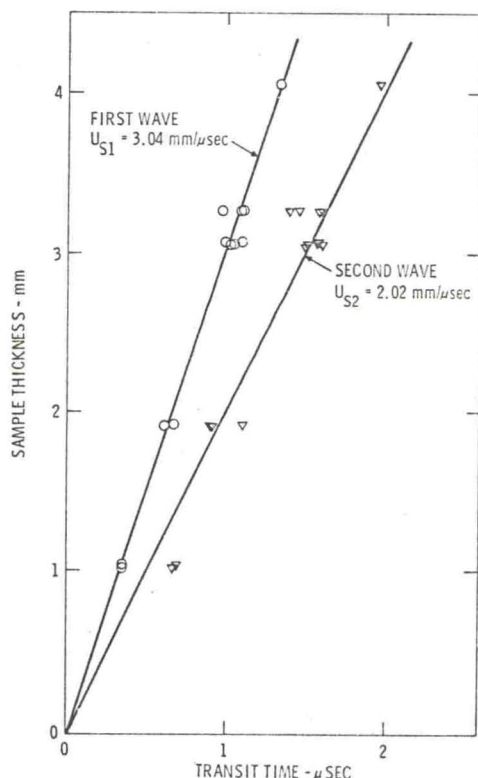
^a Stress amplitude of first precursor wave as recorded in the quartz gauge.^b Transit time of first precursor wave.^c Amplitude of second precursor wave as recorded in quartz gauge.^d Transit time of second precursor wave.

FIG. 1. Sample-thickness-transit-time graph for first two waves in 12.64 g/cm³ porous tungsten obtained for experiments where the input-stress level was varied between about 10 and 60 kbar.

The first consisted of placing the constituent parts of the target assembly in a Plexiglas cup and then encapsulating the entire assembly in an epoxy resin while the sample and gauge were held firmly together. For the second method, the porous tungsten sample was adhered to the gauge with a bead of rather viscous conducting silver paint around the periphery of the sample-gauge interface. The former method proved to be the better of the two for examining the early portions of the transmitted wave profile because intimate contact between the gauge and sample was maintained throughout the experiment. The second method was used primarily to examine the latter portions of the wave profiles since the bond was not sufficiently strong to ensure intimate contact at the sample-gauge interface when the target assembly was placed at the muzzle end of the evacuated gun barrel. The result of this poor contact was that the target gauge would start recording wave profiles at random times between the expected arrival time of the first wave and some time after the expected arrival time of the second wave. It is estimated that a separation of as little as 10⁻⁴ cm at the sample-gauge interface will cause the first wave to be completely missed and the second wave to be ambiguously recorded. The latter portions of the recorded wave profiles were essentially identical for both methods. It should be pointed out that the presence of the epoxy around the periphery of the sample in the first method had no detrimental effect on recorded wave profiles since the

TABLE II. Data pertinent to the main shock wave in 12.64 g/cm³ porous tungsten as determined from measured wave velocities.

| Projectile facing or driver plate | Proj. vel. or U_0 in driver plate (mm/ μ sec) | Sample thickness (mm) | U_{03} (mm/ μ sec) | u (mm/ μ sec) | P_3 (kbar) | V_3 (cm ³ /g) |
|-----------------------------------|---|-----------------------|--------------------------|---------------------|--------------|----------------------------|
| Quartz | 0.199 | 1.05 | 0.670 | 0.121 | 11.9 | 0.0656 |
| Quartz | 0.201 | 1.91 | 0.679 | 0.121 | 12.1 | 0.0657 |
| Quartz | 0.269 | 1.05 | 0.717 | 0.162 | 16.2 | 0.0619 |
| Quartz | 0.271 | 1.02 | 0.704 | 0.164 | 16.2 | 0.0613 |
| Quartz | 0.271 | 1.92 | 0.710 | 0.164 | 16.3 | 0.0615 |
| Quartz | 0.350 | 1.05 | 0.759 | 0.208 | 21.5 | 0.0579 |
| Quartz | 0.350 | 1.91 | 0.759 | 0.208 | 21.5 | 0.0579 |
| Quartz | 0.351 | 1.04 | 0.768 | 0.208 | 21.7 | 0.0582 |
| Lucalox | 0.298 | 1.05 | 0.799 | 0.238 | 25.5 | 0.0559 |
| Lucalox | 0.350 | 1.02 | 0.859 | 0.277 | 31.4 | 0.0540 |
| Lucalox | 0.395 | 1.06 | 0.938 | 0.308 | 37.7 | 0.0535 |
| Lucalox | 0.450 | 1.94 | 0.971 | 0.348 | 43.9 | 0.0511 |
| Lucalox | 0.503 | 1.91 | 1.07 | 0.381 | 52.7 | 0.0513 |
| Lucalox | 0.548 | 1.95 | 1.18 | 0.405 | 61.4 | 0.0522 |
| Plex-Brass ^a | 4.44 | 3.09 | 1.66 | 0.563 | 118 | 0.0523 |
| Brass ^b | 4.57 | 3.10 | 1.90 | 0.652 | 157 | 0.0519 |
| Aluminum ^c | 6.96 | 3.10 | 2.62 | 0.911 | 302 | 0.0516 |
| Aluminum ^d | 7.46 | 3.05, 4.04 | 2.93 | 1.17 | 434 | 0.0475 |
| Aluminum ^e | 8.70 | 3.01, 4.01 | 4.16 | 1.70 | 892 | 0.0469 |
| Aluminum ^f | 9.05 | 3.05, 4.01 | 4.49 | 1.84 | 1045 | 0.0467 |

^a Explosive experiment—driver plate consisted of a Plexiglas plate bonded to a brass plate with the sample placed on the brass side of the composite plate—Baratol explosive.

^b Explosive experiment—Baratol explosive.

^c Explosive experiment—TNT explosive.

^d Explosive experiment—Comp. B explosive.

^e Explosive flying-plate experiment—free run distance 1.25 cm.

^f Explosive flying-plate experiment—free run distance 2.50 cm.

pores of the tungsten were noninterconnecting, so seepage into the interior portions of the samples was negligible. This was verified by examining the interior of some samples that had been placed in an epoxy resin.

The high-explosive experiments were performed exactly as those of Ref. 2 except for lower-stress cases where the precursor waves were not overdriven. Here, the arrival of the main shock wave was detected by using quartz gauges rather than the ferroelectric crystals used at higher stresses. The driver plates used for all explosive experiments were either 2024-T4 aluminum or 22- $\frac{1}{2}$ H brass.

The porous tungsten samples used in both the gas gun and explosive experiments were all cut from a single block of material whose density was determined by weighing and measuring a cube of the material approximately 3 cm on a side. Separate measurements on samples actually used indicated that the variation in density was about $\pm 0.5\%$. The samples used in the experiments were approximately 3-cm square and ranged in thickness from about 1 to 4 mm. Their

surfaces were made flat and parallel by grinding with a diamond wheel and then dry lapping on a rotating table covered with abrasive paper. The resulting samples were parallel to within about 0.005 mm and each surface was flat to within about 0.001 mm.

RESULTS OF EXPERIMENTS

The recorded wave profiles for the porous tungsten of this study were essentially like those of the sintered porous copper of Ref. 2. A small precursor was first observed, followed by a second precursor of greater amplitude and then the arrival of the main shock wave. Arrival times of the second precursor and the main wave were measured at the half-stress points while the arrival of the first precursor was measured at the time of the first detectable disturbance because of the difficulty in determining the half-stress point of such a low-level disturbance.

Transit times and wave amplitudes for the two precursor waves are listed in Table I. Figure 1 shows a plot of sample thickness versus transit time for the

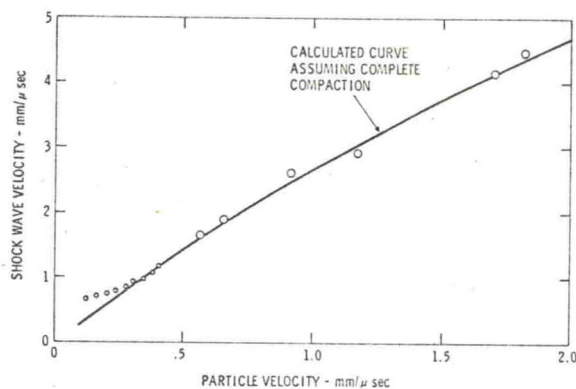


Fig. 2. Plot of main-wave shock velocities versus particle velocity for gas-gun and high explosive experiments performed on 12.64 g/cm^3 porous tungsten comparing data with predicted Hugoniot.

precursor waves, where the straight lines drawn through the data are based on least-square fits with the origin being heavily weighted to force the lines to pass through it. This was done because, when possible experimental uncertainties are considered, there is no substantial evidence that either of the two waves originate anywhere but at the impact surface. The velocity of the first wave, $3.04 \text{ mm}/\mu\text{sec}$, is in reasonable agreement with the longitudinal sound velocity of $2.95 \text{ mm}/\mu\text{sec}$ measured in the porous tungsten.

The stress levels, P_{1Q} and P_{2Q} , are those that exist in the quartz gauges and are somewhat lower than those that exist in the porous tungsten samples because of the different impedances of the two materials. The variation in values for P_{1Q} in Table I is considered to be within the limits of experimental accuracy. Thus, the data do not indicate that the value of P_{1Q} depends on either sample thickness or input-stress level. There is some scatter in the values of P_{2Q} ; however, no trends are established to indicate that its value depends on input-stress level or sample thickness either. A possible exception to this statement is that two points, obtained for samples about 1-mm thick, indicate stresses in excess of 3 kbar. This could suggest a possible dependence on sample thickness; however, the remaining data for thicker samples do not indicate a degradation in the value of P_{2Q} .

The amplitude of the second wave in the porous tungsten itself, P_2 , was determined to be 2.73 kbar. This value is based on the assumption that the porous tungsten unloads from the state behind the second wave along a mirror image of its loading line on a stress-particle velocity graph. The average value of the P_{2Q} 's of Table I along with the second-wave velocity from Fig. 1 were used in this determination. An alternative approach, namely that of assuming the porous tungsten unloads like solid tungsten, yields a value of about 3.0 kbar for P_2 . This second approach, however, is not considered to be as reasonable as the former since

the compression caused by the second wave is not sufficient to produce densities close to that of solid tungsten. The actual value of P_2 probably falls between 2.73–3.0 kbar, logically closer to 2.73 kbar. Using the first method above, the amplitude of the first wave in the porous tungsten, P_1 , is about 0.2 kbar.

The Hugoniot states behind the main wave in the porous tungsten were determined from the measured wave velocities by using the impedance-mismatch method and the Rankine-Hugoniot equations.⁷ For these calculations, the first precursor wave was neglected because it has no significant effect on the behavior at higher stresses. Values for quantities pertinent to the second wave required for this analysis are u_{p2} (particle velocity) = $0.011 \text{ mm}/\mu\text{sec}$, P_2 (stress) = 2.73 kbar, ρ_2 (density) = 12.71 g/cm^3 .

Hugoniot data pertinent to the states behind the main wave are listed in the last four columns of Table II, where U_{s3} is the main-wave velocity, u_{p3} is the particle velocity, P_3 is the stress, and V_3 is the specific volume. A shock-wave-velocity-particle-velocity representation of the Hugoniot of the porous tungsten is

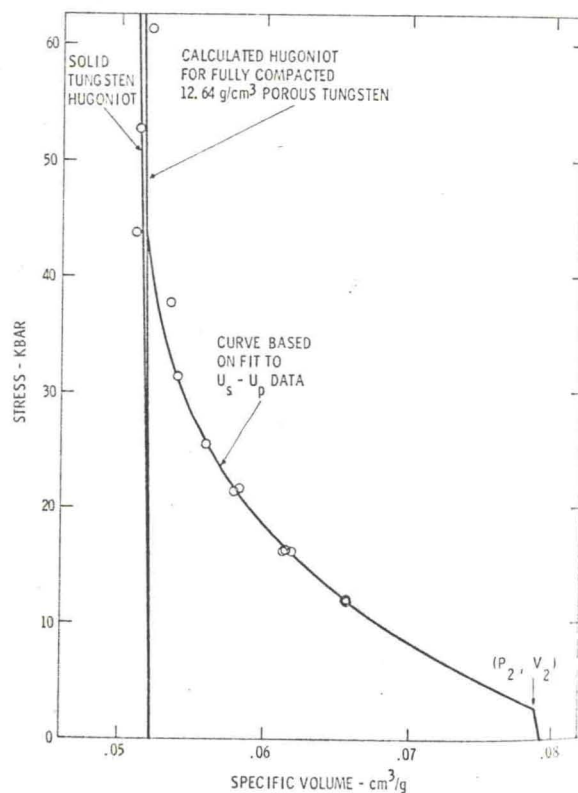


Fig. 3. Plot of stress versus specific volume for gas-gun experiments performed on 12.64 g/cm^3 porous tungsten. Also shown are the solid tungsten Hugoniot, the predicted Hugoniot of the porous tungsten, and a curve based on a fit to the shock-wave-velocity-particle-velocity data.

⁷ M. H. Rice, R. G. McQueen, and J. M. Walsh, *Solid State Phys.* **6**, 1 (1958).

shown on Fig. 2, where the solid curve represents a predicted Hugoniot, based on the assumption that the porous material is completely compacted for all stresses greater than P_2 and calculated by using the methods outlined in Ref. 2. Values for the Hugoniot parameters and Grüneisen's parameter for solid tungsten required for these calculations were taken from Refs. 8 and 9, respectively. As can be seen on Fig. 2, the higher-stress data (i.e., the data to the right on the graph) agree well with the predicted Hugoniot while the lower-stress data deviate from the calculated Hugoniot, indicating that compaction is not complete. A stress-specific volume representation of the Hugoniot of the porous tungsten in the region of incomplete compaction is shown on Fig. 3. The Hugoniot of solid tungsten is also shown on this graph along with the calculated Hugoniot of the porous tungsten assuming complete compaction. The curve drawn through the data is based on an empirical fit to the shock-velocity-particle-velocity data and indicates that complete compaction occurs at about 50 kbar.

DISCUSSION AND CONCLUSIONS

The results of this study present further verification that the Hugoniots of porous materials can be predicted for cases where complete compaction is achieved and indicate that the Hugoniots in the region of incomplete compaction gradually approach the predicted curves with increasing stress. The two precursor waves observed in the porous tungsten behave very similarly to

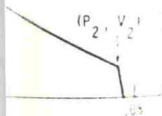
those observed in the porous copper. Both of these materials were sintered, meaning that the granules of these porous materials were rigidly held together as opposed to the rather loose binding which results from pressing powders, as was the case with the porous iron.³ The mechanisms responsible for the precursor waves are thus probably the same in both the tungsten and the copper. The model proposed in the porous copper study² to explain the two precursor waves should be equally valid for the case of porous tungsten. This model identified the first precursor wave as an elastic wave propagating through the material without significantly altering the microstructure of the porous material. The action of the second wave is to break the bonds between the granules and force them into positions such that the new specific volume is close to the minimum specific volume the granules can occupy without being significantly deformed. Since appreciable shearing occurs during this process, the velocity of the second wave is likely related to the shear-wave velocity in the material. For both the sintered porous copper and tungsten, the ratios of the first-wave velocity to the second-wave velocity are within about 15% of the ratios of longitudinal-wave velocity to shear-wave velocity for the respective solid materials. This provides some verification of the model. The lack of rigidity in the pressed iron powder³ probably prevents a detectable first precursor wave from being formed.

ACKNOWLEDGMENT

The author is indebted to S. A. Beam for his help in assembling and performing the experiments of this study.

⁸ R. G. McQueen and S. P. Marsh, *J. Appl. Phys.* **31**, 1253 (1960).

⁹ K. A. Gschneidner, *Solid State Phys.* **16**, 410 (1964).



for gas-gun experiments. Also shown is the Hugoniot of the porous material and the shock-wave-velocity

Walsh, *Solid State Phys.*